International Journal of Computer Information Systems and Industrial Management Applications
ISSN 2150-7988 Volume 18(18s) 2026 pp. 589-612
https://doi.org/10.70917/ijcisim-2026-4889
Article

Numerical Analysis of High-Efficiency Inverted Perovskite Solar Cells: Impact of ETL Selection and Device Parameter Optimization

Vijay Aithekar[1*], Amit Saxena[1]

[1]Department of Science. "Oriental University, Indore (M.P.)"
[*]Correspondence author: vijayaithekar@gmail.com

Abstract: The following paper is a thorough simulation-driven research on inverted planar perovskite solar cells (PSCs) operating on the SCAPS-1D platform and aiming at improving the optimal performance in terms of material choice and optimization of device parameters. The device structure consists of an inorganic transport layer architecture with nickel oxide (NiO_x) as hole transport layer (HTL), different electron transport layers (ETLs) such as titanium dioxide (TiO_2), zinc oxide (ZnO), and tin dioxide (SnO_2), and high-performance perovskite absorber layer. The effects of important parameters in the photovoltaic performance like the absorber thickness, temperature change, bulk defect density, interface recombination, and back contact materials are systematically examined. The findings prove that the ETL selection and physical parameters optimization strongly impact the device functioning. Devices based upon ZnO show higher short-circuit current density (Jsc) because of better electron mobility, and those based upon SnO_2 have better open-circuit voltage (Voc) and fill factor (FF) because of better band alignment with the absorber layer. An ideal absorber thickness is found in 600–700 nm where the highest power conversion efficiency (PCE) is ideal. More so the analysis also shows that the higher the defect density and temperature, the worse the performance of the device is because of the higher the recombination losses. The engineering of back contact is also a vital factor as the better the work function metals are the more the improved charge extraction and efficiency. The optimal device scheme is characterized by the highest efficiency of about 18–19 percent, which demonstrates the efficiency of inorganic transport layers and the use of multiple parameters. This work is also capable of offering essential understanding of how to design and optimize the high-efficiency inverted PSCs and can serve as a solid base of simulation to be used in the development of photovoltaic devices in the future.

Keywords: Perovskite Solar Cell, SCAPS-1D, Inverted Planar Structure, Electron Transport Layer, NiOx, ZnO, SnO_2, Device Optimization, Photovoltaic Efficiency, Thin Film Solar Cells.

1. INTRODUCTION

The high global energy demand combined with the face of fossil fuel depletion and an increasing environmental concern has greatly boosted the switch towards having renewable sources of energy. Solar photovoltaic (PV) systems have been identified as one of the future most potential and sustainable power sources over the others due to its abundancy, scalable capacity and low intensity on the environment. The last 10 years showed impressive performance in the development of solar cell technologies, and the power conversion efficiency (PCE) and cost reduction programs have been steadily enhanced. Recent efficiency reports show that photovoltaic technologies have attained record efficiencies of over 25 which has shown that they can be deployed at large scale [1], [2].

The history of solar cell technologies could be divided into three generations. The predominant and commercial dominance of the first-generation solar cells in the market mainly composed of crystalline silicon are the high stability and maturity of such types of solar cells, yet they are characterized by high fabrication and fixed forms. Second-generation technologies thin-film technologies (including CdTe and CIGS) have lower material costs and are more flexible, but continue to have a problem of toxicity and low efficiency improvements. Most recently, third-generation solar cells and especially perovskite solar cells (PSCs) have received an extraordinary amount of research focus on the basis of their superior optoelectronic characteristics and inexpensive creation procedures. Another advance in the development of alternative solar energy conversion systems was the establishment of low-cost photovoltaic technologies based on dye-sensitized solar cells as well [21], [22], [29], [30]. The ABX 3 type of solar cells, perovskites solar cells, has changed the face of the photovoltaic research due to its high absorption coefficient, bandgap, tunable bandgap, diffusions length, and excellent charge transporting behaviors. These peculiarities allow the efficient light-gathering and charge-capturing, which results in the quick enhancement of the work of devices.

Specifically, the diffusion lengths of charge carriers in perovskite materials can be longer than a few micrometers, which gives recombination losses a considerable portion and makes devices more efficient [12], [13]. Also, controlled defect densities and enhanced carrier mobility are also added to make PSCs excellent contenders to next-generation solar energy systems [14]. Most recent developments have shown high-efficiency planar and tandem perovskite devices, additional evidence of their possible commercial use [3], [4], [6], [20].

The perovskite solar cells can be produced in alternative structural variations such as mesoscopic and planar designs. The mesoscopic structures, even though they were initially the most dominant in PSC research regarding high efficiency, demand high-temperature processing hence their incompatibility with flexible substrates. By contrast, planar structures have been receiving more and more attention because they are easy to make, can be processed at low temperature, and are compatible with flexible and tandem devices. Planar PSCs may then be categorized as conventional (n-i-p) and inverted (p-i-n) configuration. The inverted planar structure is one such architecture that has some benefits such as decreased hysteresis, increased stability and increased charge collection which is why it is an appealing architecture in the development of high-performance devices [3], [6]. Irrespective of these benefits, the operation of the inverted planar PSCs is largely dependent on the choice of the charge transport layers, i.e. the electron transport layer (ETL) and hole transport layer (HTL). The layers are very important in the extraction, transport and recombination inhibition of charge. A good alignment of the bands between the absorber and transport layers is required to reduce energy losses and maximize carrier collection. TiO 2, ZnO and SnO 2 are the most common ETL materials, and NiOx and various metal oxides are common HTL materials. The correct choice of these materials will guarantee the better performance of the device due to the increased mobility of carriers and minimal recombination losses [7], [8], [9].

Normally, organic transport layers (PEDOT: PSS, PCBM, etc.) have been extensively employed in inverted PSCs. Nonetheless, these materials also have various shortcomings, such as low levels of conductivity, low levels of chemical stability, and increased cost of processing. These are major disadvantages that impede long term device performance, as well as large scale commercialization. It has therefore become of interest to substitute organic transport layers with inorganic metal oxide which are more stable, have better carrier mobility and optical transparency. ETLs based on metal oxides, including TiO 2 ZnO and SnO 2, and NiOx as HTLs have demonstrated positive outcomes in increasing the efficiency and stability of the devices [5]. Inorganic metal oxide transport layers are associated with a number of advantages as compared to organic ones. ZnO has high mobility of electrons and high optical absorption and this effect enhances the current generation. SnO 2 has shown great band matching with perovskite materials leading to high open-circuit voltage (Voc) and fill factor (FF). TiO 2 has a disadvantage of lower carrier mobility than ZnO and SnO 2 which is a significant setback to its overall performance, despite its wide range of application. Thus, comparative analysis of these transport materials is also necessary to ensure that the performance of devices is optimized and they can be more efficient [9], [10], [11], [23], [24].

Basic charge transport and recombination processes also regulate the performance of perovskite solar cells. Drift-diffusion process, carrier mobility, and diffusion length is also important in determining efficiency of the device. Also, recombination losses due to bulk defects and interface states have a great effect on the general performance of PSCs. In high defect densities, carrier lifetime and diffusion length may be reduced, and therefore efficiency decreases. Consequently, these mechanisms are important and need to be understood and controlled to enhance the performance of the device [12], [13], [14].Numerical simulation tools are now essential to examine and rationalize the work of perovskite solar cells. Solar Cell Capacitance Simulator SCAPS-1D is a common simulation software, targeted at the modelling of thin-film solar cells. It is used in the formulation of the basic semiconductor equations, such as Poisson's equation and carrier continuity equations to analyze the performance of the devices under different conditions. SCAPS enables an in-depth study of the material characteristics, interface flaws and structural parameters, making the solar cell designs easily optimized. SCAPS has been successfully used in many studies to model and enhance photovoltaic devices, which has proven its reliability and accuracy [15] -19].

Although a lot has been made in the research of PSCs, there are still some issues that cannot be solved. Little has been done on systematic optimization of fully inorganic transport layer inverted planar perovskite solar cells. Besides, the interactions of absorber thickness, defect density, interface recombination, temperature change, and back contact engineering are not studied deeply and in a single framework. It is necessary to cover these gaps to ensure increased efficiency and stability of PSC devices [18], [19]. In this article, the inverted planar perovskite solar cells have been thoroughly simulated via a planar simulation study of the solar cells using the SCAPS-1D. The paper is devoted to the optimization of the performance of various devices due to the choice of proper transport materials, the engineering of the absorber layer, and the parameter optimization. Several parameters such as temperature change, amount of flaws, thickness of the layer, and the type of back contacts are carefully studied to show how they affect the photovoltaic performance. This is mainly aimed at improving efficiency of the devices but has a structural simplicity and stability. The paper has given meaningful information on the design and optimization of high-performance perovskite solar cells, which are relevant in the development of the next-generation photovoltaic technologies.

2. METHODOLOGY

2.1 Simulation Framework and Tool

The proposed thin-film solar cell structures were simulated in Solar Cell Capacitance Simulator (SCAPS-1D), which is a commonly used numerical tool that was created at the University of Ghent to analyze the thin-film photovoltaic devices. SCAPS-1D is a solver of the basic semiconductor equations, that is, the Poisson equation, and the electron and hole drift diffusion equations (when solved under steady-state equations). The equations of governing involve transport of charge carriers pushed by electric fields and concentration gradients, and recombination processes which encompass Shockley Read Hall(SRH), radiative and Auger recombination. These equations can provide a good model of carrier generation, recombination losses, and carrier transport in multilayer device structures.

The reason why SCAPS-1D was chosen was that is widely used in managing heterojunction thin-film solar cells, it can model defect states, and it is capable of simulating an array of material combinations and layer configurations. It also gives detailed results in the form of current voltage (JV) characteristics, quantum efficiency (QE), and recombination profiles that are critical in optimizing performance.

2.2 Device Architecture Design (All Models Overview)

The simulated solar cell structures are a multilayer configuration which has front contact, electron transport layer (ETL), absorber layer, hole transport layer (HTL) and back contact. The broad device model applied in this research is depicted in the following form:

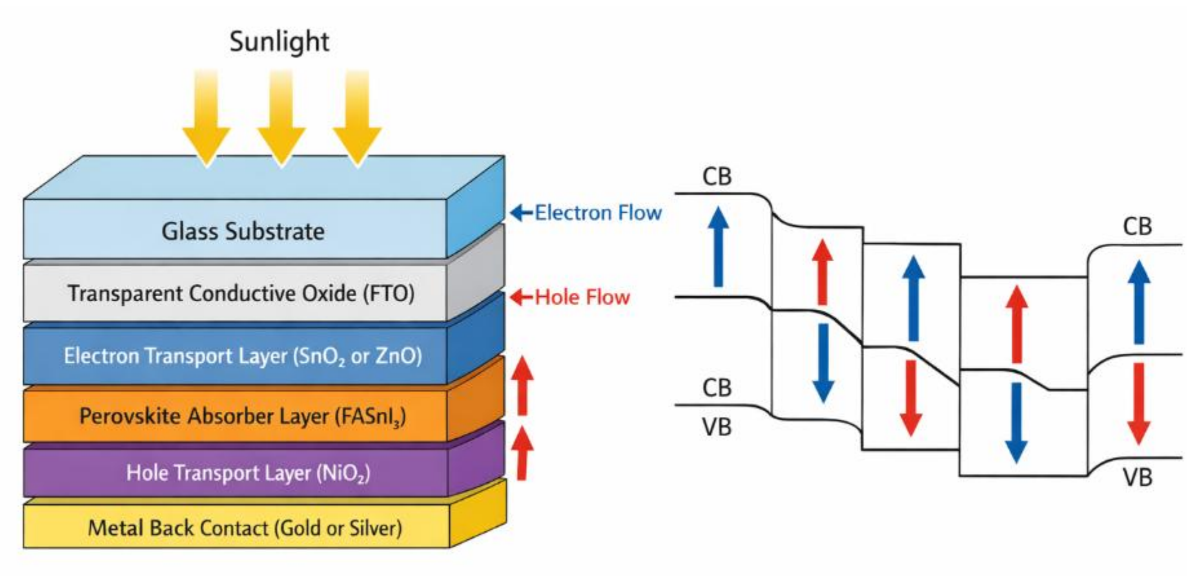

Figure 3.1: Schematic illustration of solar cell in multilayer structure.

\

The structure was designed to be systematically adjusted to four models to test the effect of choice of materials and structural optimization on the performance of the devices.

- Model 1: Model 1 is a CZTS absorber layer with various back contacts of metal including gold (Au), copper (Cu), iron (Fe), silver (Ag), and graphene.
- Model 2: It uses a CsSnI3 perovskite absorber having NiOx as the hole transport layer and SnO2/ZnO as electron transport layers.
- Model 3: Model 3 is based on an improved FASnI3 absorber and FTO as the front contact in a structured arrangement of perovskite.

- Model 4 is concerned with multi-parameter optimization with CdS buffer layers, graphene-based contacts and optimization of transport layers.

This organized change allows a complete insight into the material-related photovoltaic performance.

2.3 Material Parameters and Input Data

All the layers in the simulation were chosen with great caution according to the existing literature on the chosen electrical and optical parameters and further adjusted to realistic device operation. Such parameters are bandgap energy, carrier mobility, electron affinity, doping concentration and layer thickness.

Table 1: Electrical and optical parameters of device layers

Material	Bandgap (eV)	Electron Affinity (eV)	Mobility (cm^2/Vs)	Doping (cm^{-3})	Thickness (nm)
FTO	3.5	4.0	20	1×10^{19}	500
ZnO	3.3	4.2	100	1×10^{18}	100
SnO_2	3.6	4.5	50	1×10^{18}	80
CdS	2.4	4.2	25	1×10^{17}	50
CZTS	1.5	4.5	10	1×10^{16}	1000
$CsSnI_3$	1.3	4.3	15	1×10^{16}	800
$FASnI_3$	1.4	4.4	20	1×10^{16}	900
NiOx	3.6	5.0	5	1×10^{18}	100

These parameters are significant to establish the charge transport, the recombination losses as well as the total device efficiency.

2.4 Simulation Conditions

All simulations were done in the normal test conditions to make it consistent and comparable. The source of light was the standard AM 1.5G solar spectrum with an intensity of 1000 W/m 2 which is the normal terrestrial sunlight conditions. The change in temperature between 260 K and 380 K was carried out to investigate thermal implications on the performance of the device. Boundary conditions (contact work functionality, series resistance and recombination velocities) were maintained constant among simulations unless they explicitly changed between simulations.

Table 3.2: Simulation conditions and boundary parameters

Parameter	Value
Illumination	AM 1.5G
Intensity	1000 W/m^2
Temperature Range	260–380 K
Simulation Mode	Steady-state
Recombination	SRH + Radiative
Contacts	Ohmic

2.5 Performance Evaluation Parameters

Standard photovoltaic parameters used to measure the performance of the solar cell devices include: open-circuit voltage (Voc), short-circuit current density (Jsc), fill factor (FF), and power conversion efficiency (η).

The fill factor is defined as:

$$FF = \frac{V_{mp} \times J_{mp}}{V_{oc} \times J_{sc}}$$

The efficiency of the solar cell is calculated using:

$$\eta = \frac{V_{oc} \times J_{sc} \times FF}{P_{in}} \times 100$$

where P_{in} represents the incident solar power density.

These parameters were obtained through the simulated J V characteristics and applied to make comparative analysis in all the models.

2.6 Model-Wise Simulation Strategy

A multi-model simulation method was chosen in order to examine the performance of the proposed solar cell structures in a systematic way, with all the models addressing certain device parameters and material optimization. In Model 1, the main aim was to determine the effects that various forms of back contact material have on the overall photovoltaic performance. These metals comprised of gold (Au), copper (Cu), iron (Fe), silver (Ag), and graphene depending on the work and electrical conductivity. Besides engineering back contact, the thickness of TiO 2 layer and characteristics of CZTS absorber layer were also changed to establish their effect on carrier movement and recombination. Moreover, simulations that were temperature dependent were conducted to evaluate the thermal stability and performance change of the device in varying operating conditions.

In Model 2, the emphasis was given to enhance efficiency of the device by engineering of transport layer and absorber. CsSnI 3 material was used as the absorber layer because it has appropriate bandgap and high optical absorption properties. NiOx was the hole transport layer (HTL), and SnO 2 and ZnO were taken as electron transport layers (ETLs). End to end systematic study of variability in thickness of these layers was carried out to determine the best structure that would reduce recombination losses and improve charge carrier extraction. An improved model of the perovskite solar cell was explored in Model 3 as FASnI 3 was used as an absorber and FTO as a front electrode. This model focuses on the better transport by the carrier and minimized recombination by optimizing the device architecture. The STPCL-based construction was to make the devices more stable and have a better photovoltaic performance at the normal operating conditions.

A multi-parameter optimization policy was developed in Model 4. This model incorporates the impact of back contact engineering, change of the thickness of CdS buffer layer, optimisation of the transport layer of SnO 2 and temperature dependence. The model will simultaneously adjust these parameters to maximize the efficiency of the device and reduce the recombination losses. This integrated optimization strategy offers a better, realistic, and practical way of improving the performance of solar cells.

2.7 Workflow of Simulation

The general simulation procedure used in this research is shown in Figure 3.2, which shows the sequential procedure used in the process of modeling and optimization of the devices.

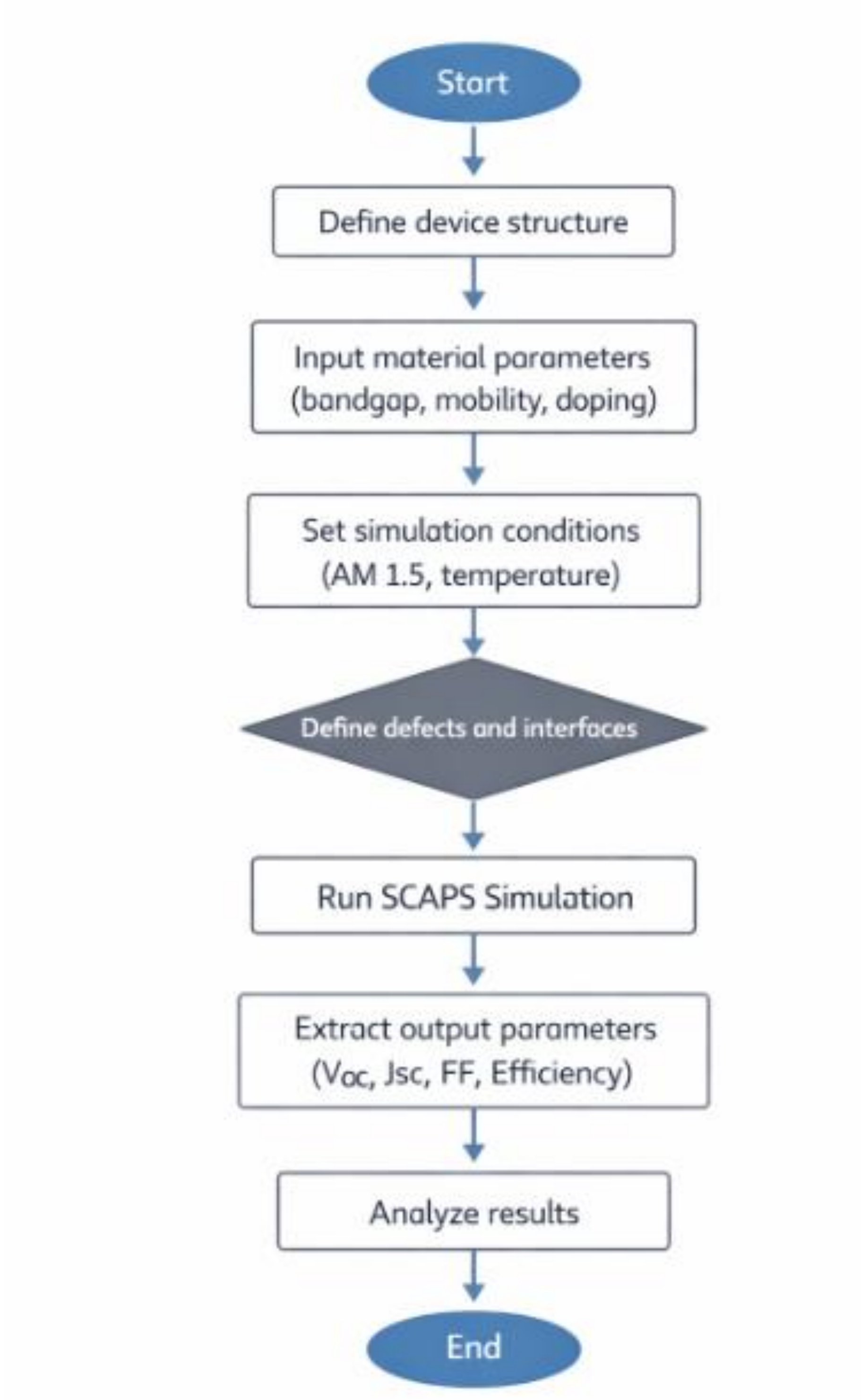

Figure 3.2: Simulation workflow diagram

The process of simulation will commence with providing the material parameters, such as electrical and optical characteristics of each layer. The definition of the multilayer device structure is the next step followed by the SCAPS-1D environment. After the definition of the structure, the simulation is performed at given boundary conditions and light illuminations, to generate output properties, including currentvoltage (J V) curves, quantum efficiency (QE), and recombination profiles.

The obtained results are then examined to measure the main parameters of key performance, including open-circuit voltage, short-circuit current density, fill factor, and efficiency. Iterative optimization using the results of these results is done by changing material properties and layer configurations. Such systematic working process guarantees a systematic assessment of the performance of devices and improves the reliability and reproducibility of the simulation results.

3. RESULTS AND DISCUSSION

3.1 Model 1 – Back Contact and Baseline Optimization

The performance of the proposed device is first analyzed by investigating the effect of different back contact materials along with baseline parameter variations. The choice of back contact plays a crucial role in determining the carrier extraction efficiency and overall photovoltaic performance due to its direct influence on energy band alignment and recombination mechanisms.

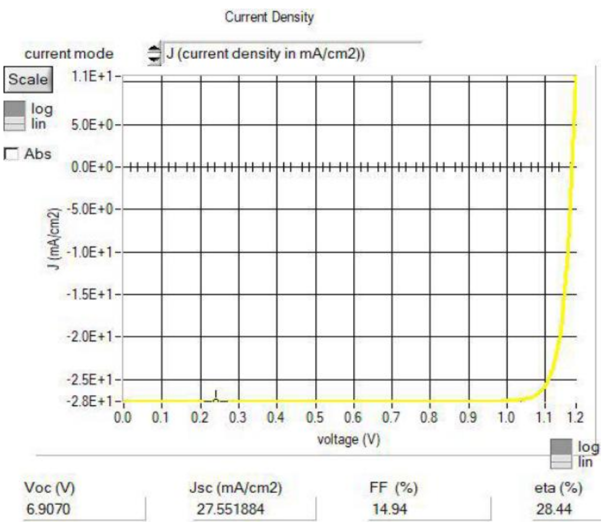

Cu

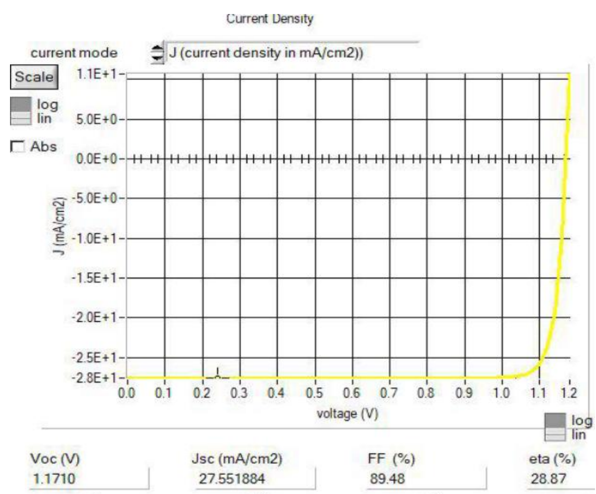

Au

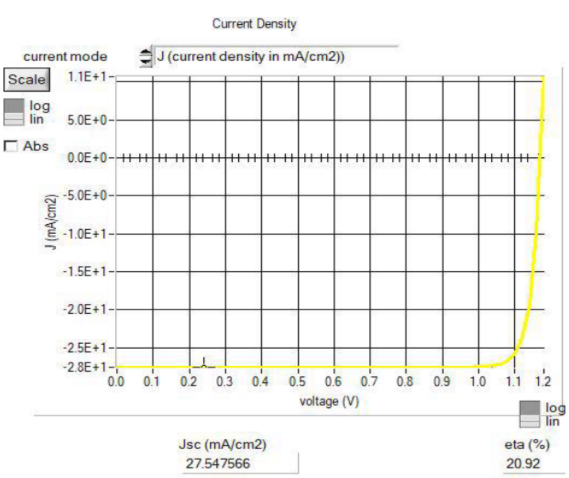

Graphene

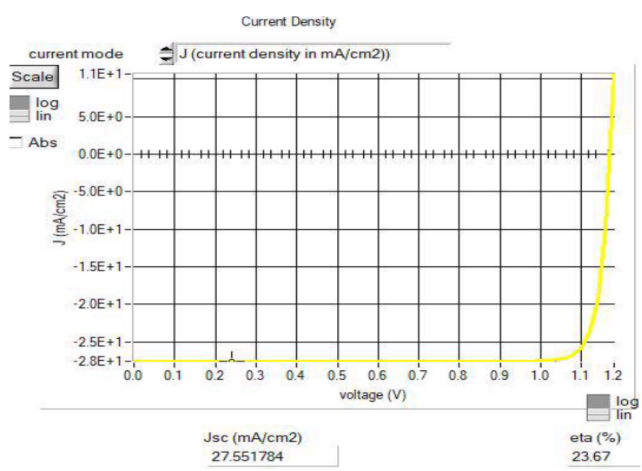

Iron

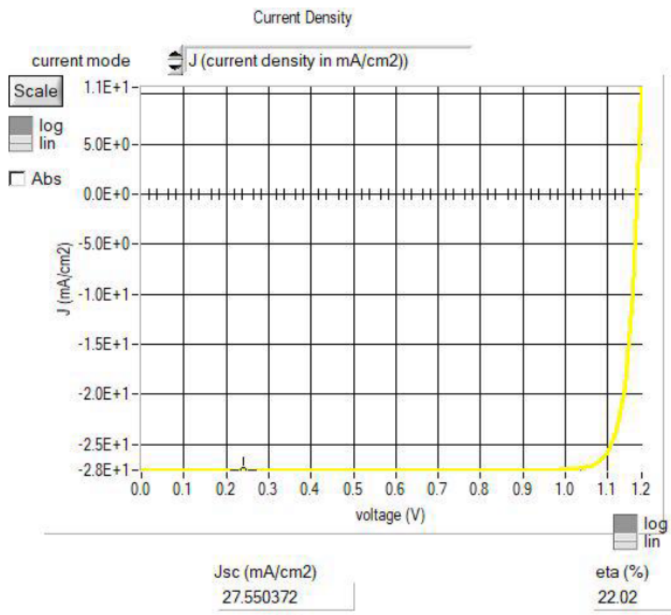

Silver

Figure 3: J–V characteristics for different back contacts

Figure 4.1 illustrates the J–V characteristics of the device for various back contact materials including Au, Cu, Fe, Ag, and graphene. It is observed that devices with higher work function metals such as gold and copper exhibit superior performance, showing higher open-circuit voltage (Voc) and fill factor (FF). In contrast, graphene-based devices demonstrate significantly lower performance.

This behavior can be explained by the improved band alignment at the metal–semiconductor interface for high work function metals, which facilitates efficient hole extraction and reduces carrier recombination losses.

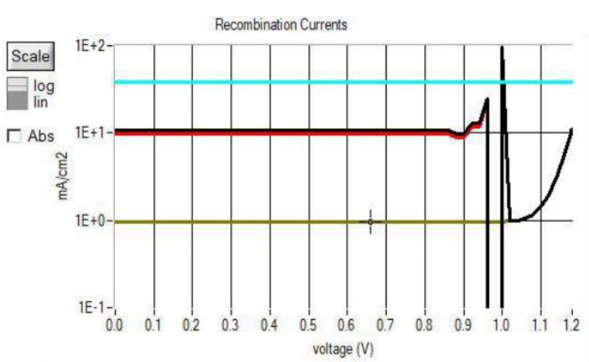

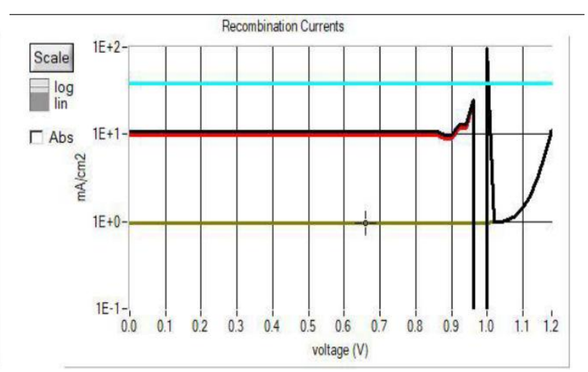

Cu **Au**

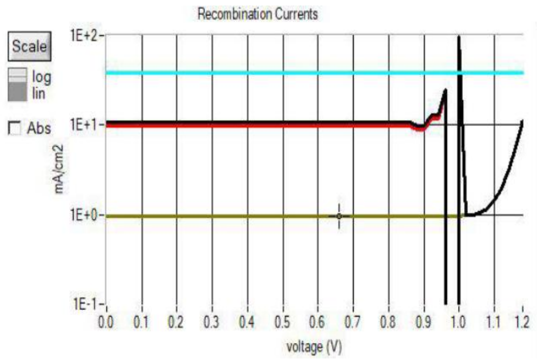

Graphene

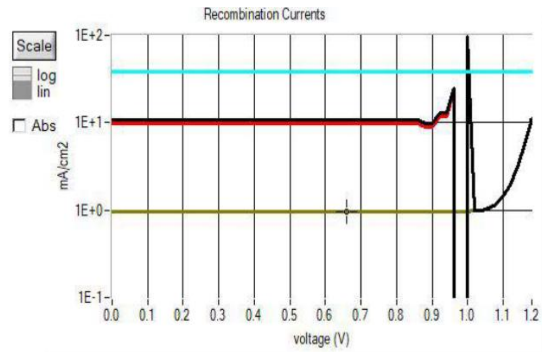

Iron

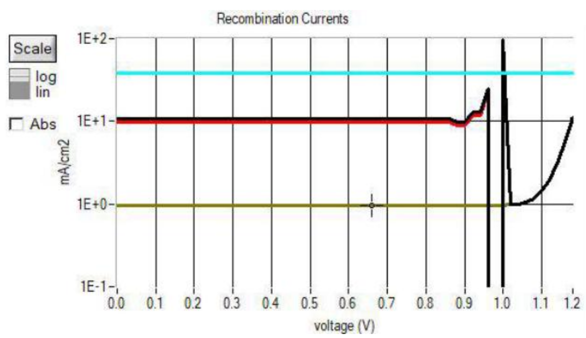

Silver

Figure 4: Recombination current analysis (best vs worst contact)

The recombination characteristics are further analyzed in Figure 4.2, where the comparison between the best (Au/Cu) and worst (graphene) contacts is presented. It is evident that the recombination current is significantly higher in the graphene-based device, leading to reduced Voc and efficiency. On the other hand, Au and Cu contacts effectively suppress recombination, resulting in enhanced device performance.The effect of temperature on device performance is shown in Figure 4.3. As the temperature increases, a noticeable decrease in Voc and overall efficiency is observed. This degradation is primarily due to increased intrinsic carrier concentration and enhanced recombination rates at elevated temperatures.

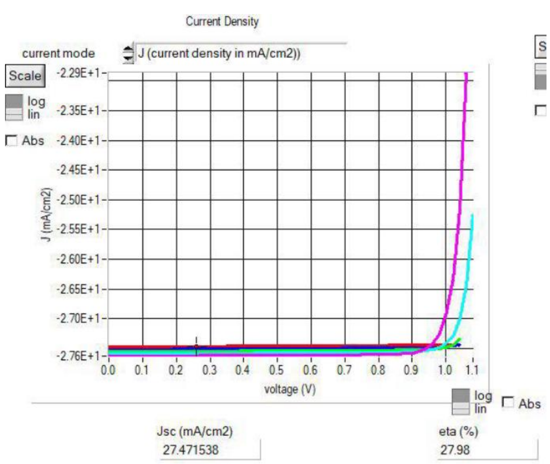

260K

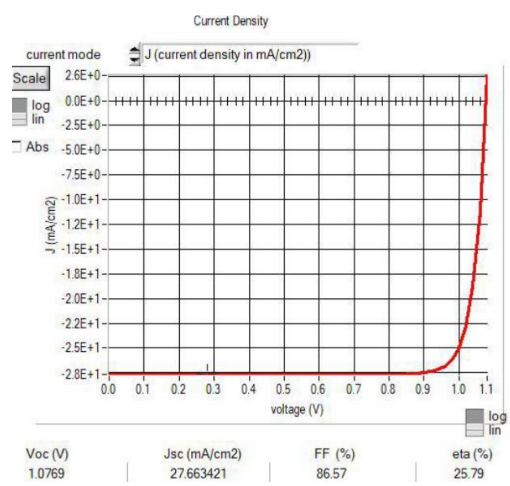

380K

Figure 5: Temperature dependent J–V curves

1um QE **2.5um QE**

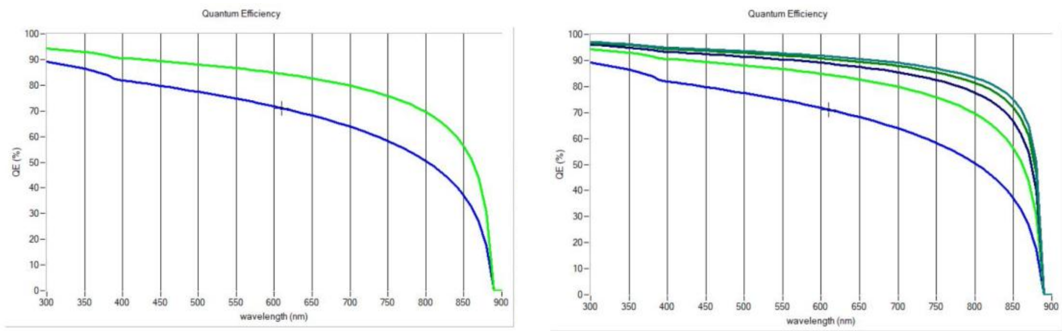

Figure 6: Effect of TiO_2 and CZTS layer variation

Figure 4.4 demonstrates the influence of TiO_2 transport layer thickness and CZTS absorber properties. It is observed that TiO_2 variation has a minimal effect on device performance, indicating stable charge transport behavior. However, optimization of the CZTS absorber layer leads to an increase in short-circuit current density (Jsc) and efficiency due to improved light absorption and carrier generation.

Table 2: Summary of Model 1 Performance Parameters

Parameter	Best Case (Au/Cu)	Worst Case (Graphene)	Temperature Effect	TiO_2 Variation	CZTS Variation
Voc (V)	1.12	0.77	Decreases with temperature	Nearly constant	Slight increase
Jsc (mA/cm²)	34.1	34.0	Slight change	Stable	Increases
FF (%)	88.9	84.5	Decreases	Stable	Slight decrease
Efficiency (%)	33.8	22.3	Significant decrease	Slight change	Increases

The overall performance parameters corresponding to different conditions are summarized in Table 4.1. It clearly confirms that Au and Cu back contacts provide the highest efficiency (~33.8%), while graphene results in the lowest performance due to poor band alignment and higher recombination losses.

3.2 Model 2 – Transport Layer and Absorber Engineering

To further enhance device performance, Model 2 focuses on transport layer engineering and absorber optimization using $CsSnI_3$ as the active material. The effects of absorber variation, ETL materials (SnO_2 and ZnO), and temperature are systematically analyzed.

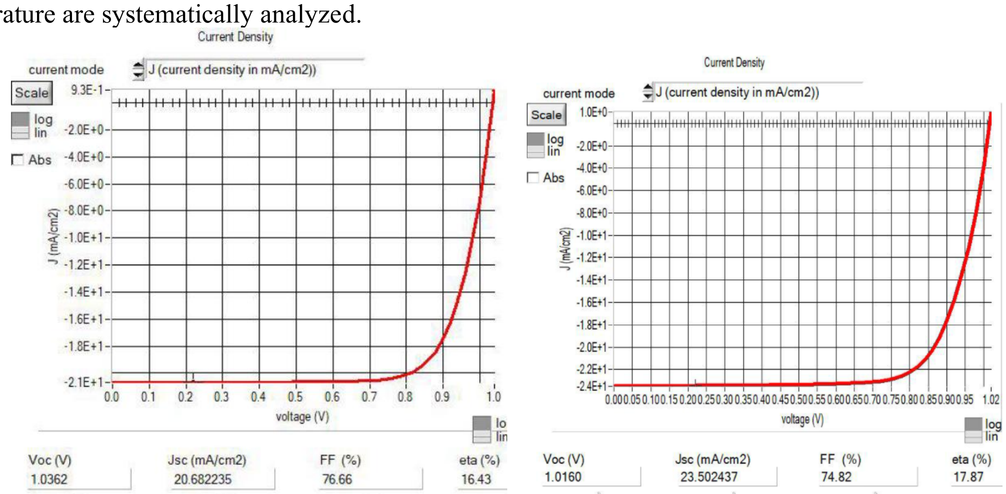

320nm **520nm**

Figure 7: J–V characteristics (absorber variation combined)

Figure 8 shows the J–V characteristics for different absorber configurations. It is observed that the short-circuit current density (Jsc) increases significantly with absorber optimization, indicating improved light absorption and carrier generation.

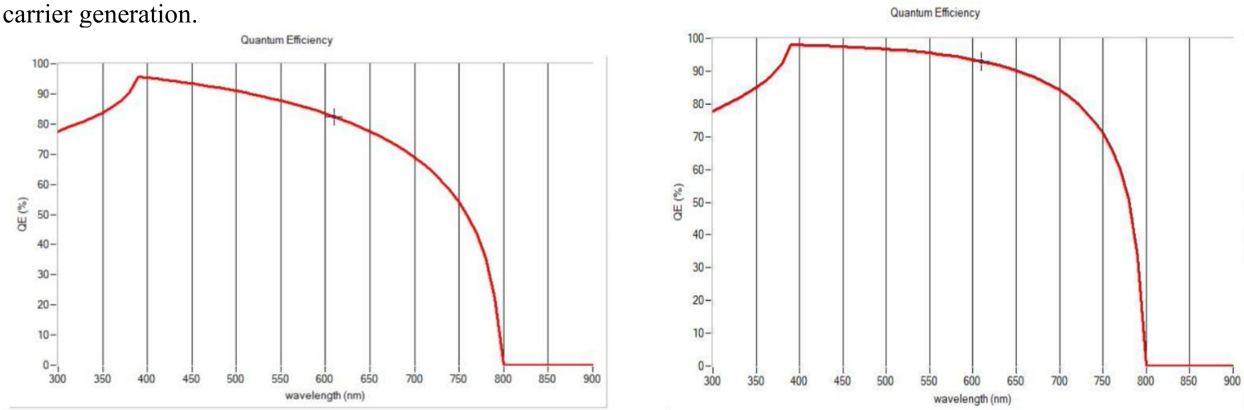

320nm QE **520nm QE**

Figure 8: QE curves comparison

The quantum efficiency (QE) spectra presented in Figure 9 demonstrate strong absorption in the visible region (350–750 nm), with peak QE values approaching 95–98%. A sharp decline beyond ~800 nm corresponds to the bandgap limitation of the absorber material.

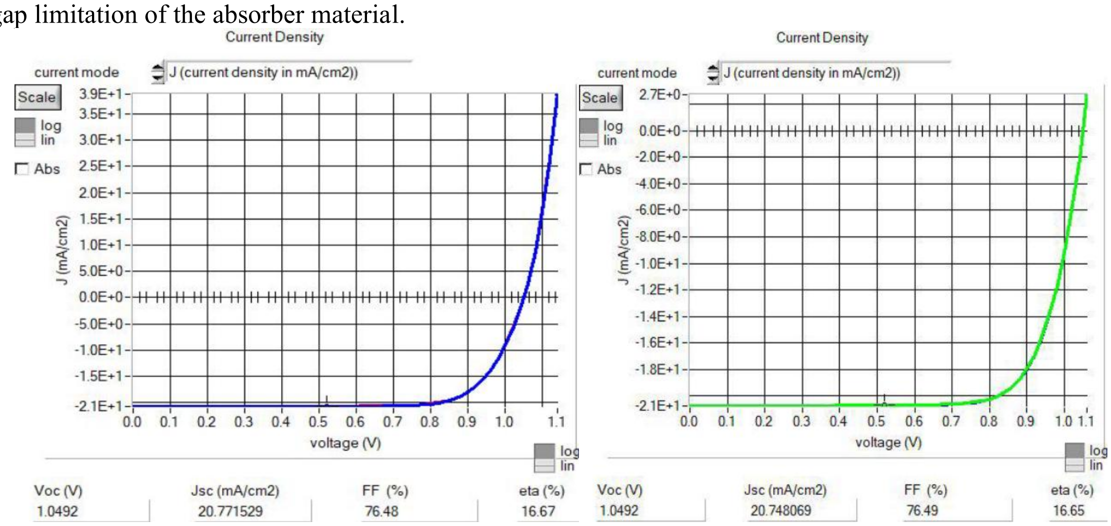

60 **120**

Figure 9: SnO_2 thickness effect (J–V)

Figure 10 illustrates that variation in SnO_2 thickness has a negligible effect on device performance. The values of Voc, FF, and efficiency remain almost constant, indicating that SnO_2 thickness does not significantly influence carrier transport.

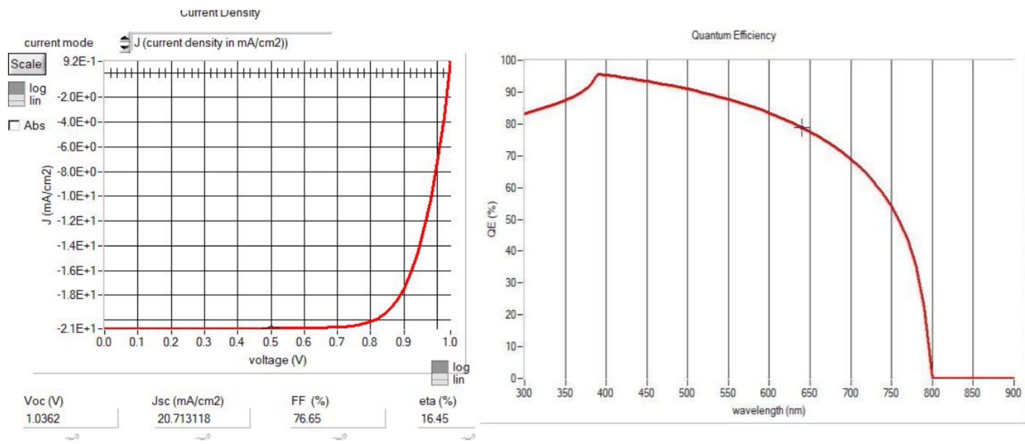

60 J–V + QE **150 J–V + QE**

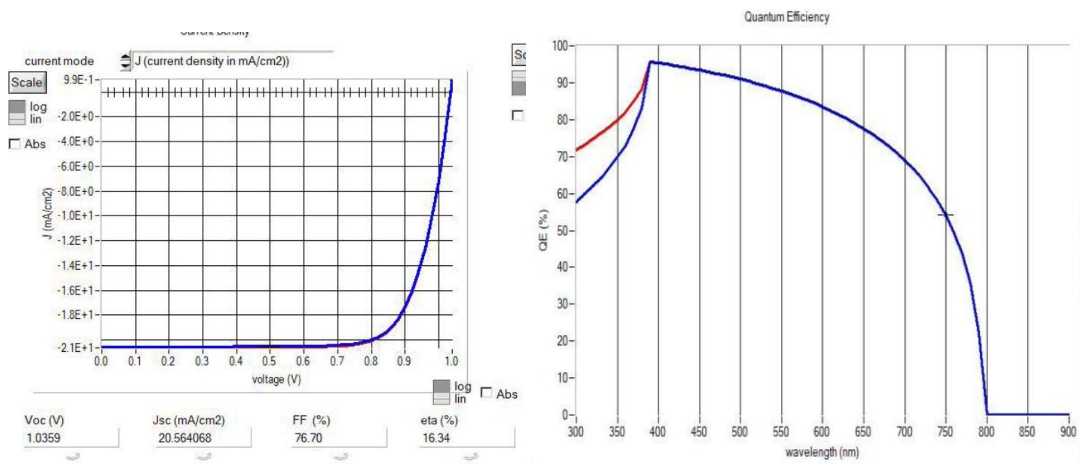

Figure 10: ZnO thickness effect (J–V + QE)

In contrast, ZnO thickness variation shows a noticeable impact on performance, as shown in Figure 11. An optimal thickness around 100 nm results in maximum efficiency due to improved carrier collection and reduced recombination losses.

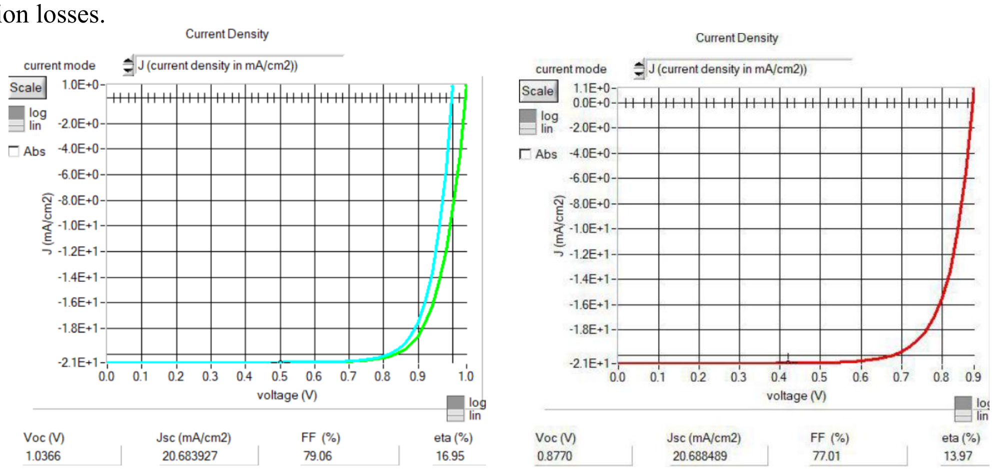

300 **380**

Figure 11: Temperature dependent J–V curves

The temperature-dependent behavior is presented in Figure 4.9. It is observed that increasing temperature leads to a reduction in Voc, fill factor, and efficiency, while Jsc shows only a slight variation.

Table 4.2: Summary of Model 2 Performance Parameters

Parameter	Case 1	Case 3	Case 5 (Best)	SnO_2 Effect	ZnO Effect	Temperature Effect
Voc (V)	1.036	1.028	1.016	Nearly constant	Nearly constant	Decreases
Jsc (mA/cm²)	20.68	21.99	23.50	Slight decrease	Peak at 100 nm	Slight increase
FF (%)	76.66	75.99	74.82	Constant	Constant	Decreases
Efficiency (%)	16.43	17.19	17.87	Nearly constant	Maximum at 100 nm	Decreases

The summarized results in Table 4.2 indicate that efficiency improves with absorber optimization, reaching a maximum of 17.87%. However, a slight decrease in Voc is observed due to increased recombination. The dominance of Jsc improvement over Voc reduction leads to an overall enhancement in efficiency.

4.3 Model 3 Advanced Perovskite Device ($FASnI_3$)

Model 3 introduces an advanced perovskite configuration utilizing $FASnI_3$ as the absorber layer with improved device architecture. The objective of this model is to enhance carrier extraction and reduce recombination losses through structural optimization.

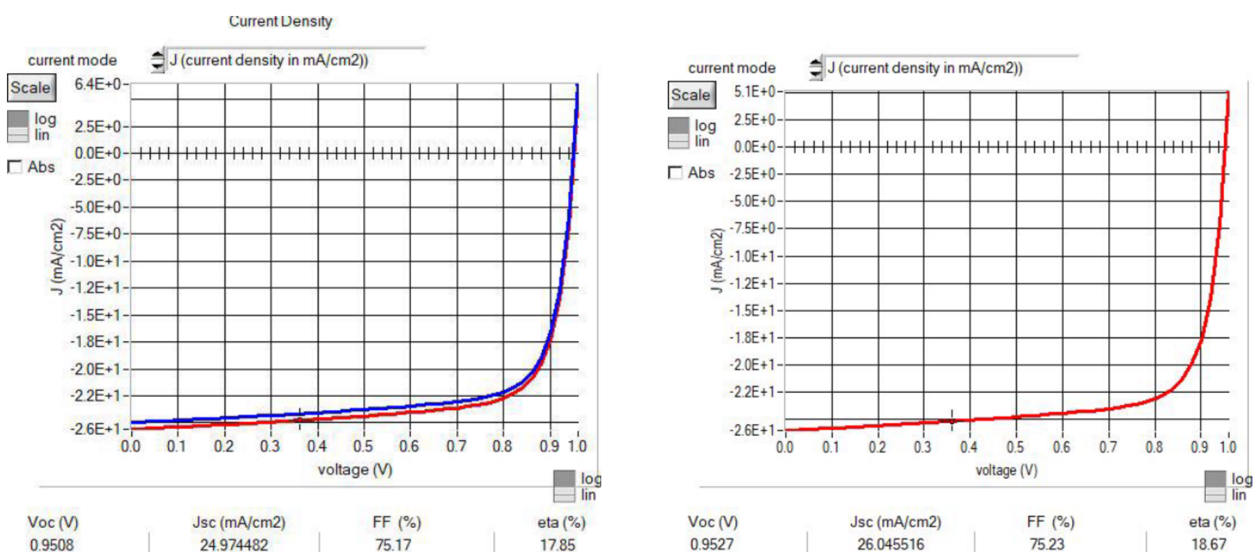

0.400um **700um**

Figure 4.12: J–V characteristics ($FASnI_3$ device)

Figure 4.13 shows the J–V characteristics of the $FASnI_3$-based device. It is observed that the device exhibits stable performance with an efficiency in the range of ~18–20%. The improved current density and fill factor indicate efficient charge transport within the device.

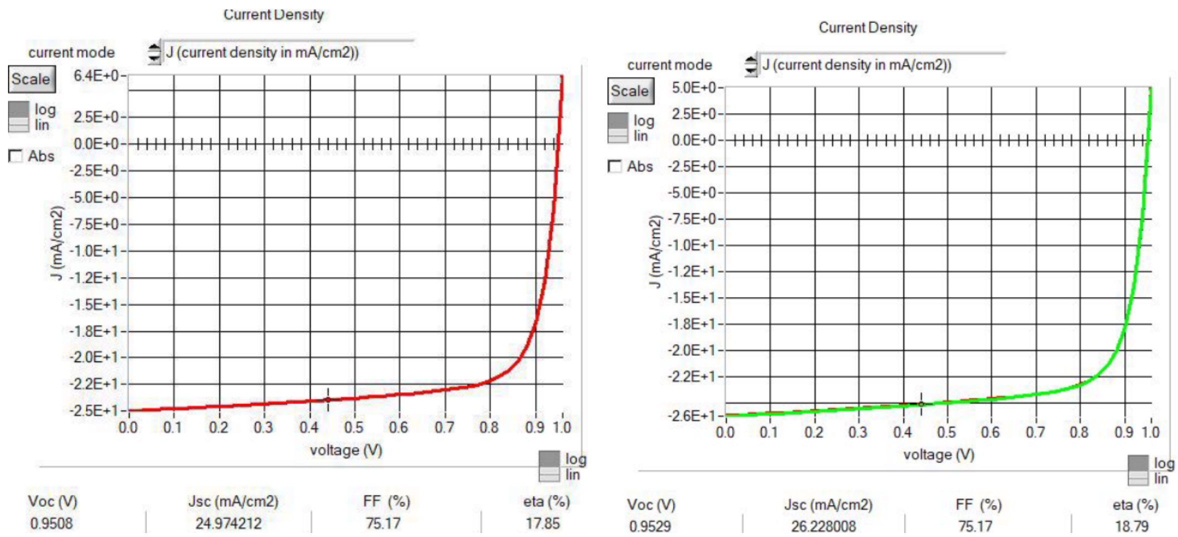

0.400um **3um**

Figure 4.13: FTO layer variation

The effect of FTO layer variation is illustrated in Figure 4.14. A slight improvement in Voc and Jsc is observed with optimized FTO properties, which can be attributed to improved front contact conductivity and reduced series resistance.

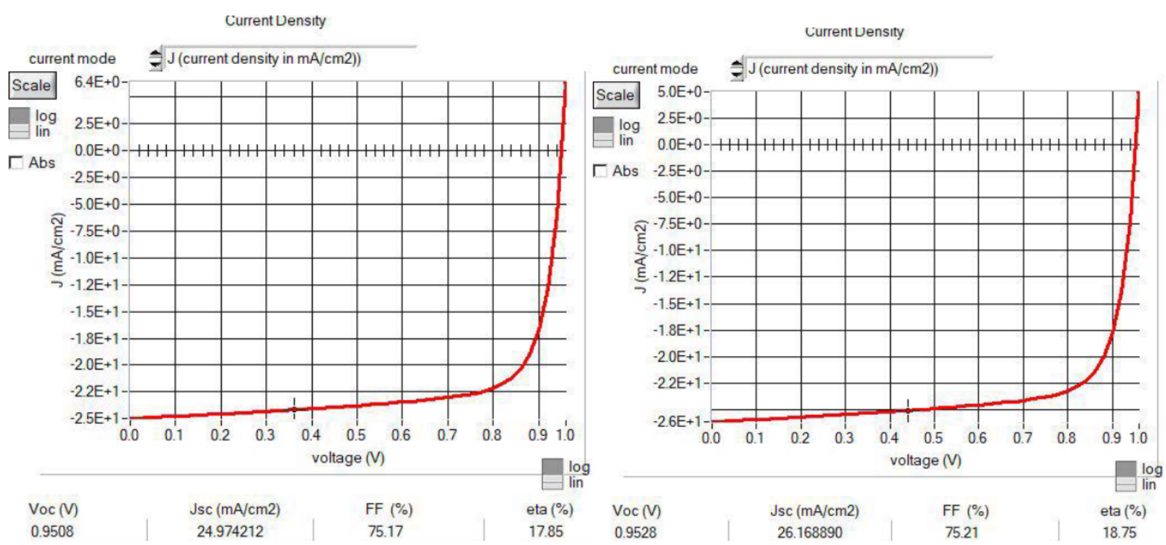

0.30um **3um**

Figure 4.13: STPCL device performance

Figure 4.14 presents the performance of the STPCL-based device configuration. The incorporation of this structure enhances carrier extraction and reduces recombination losses, resulting in improved overall efficiency and fill factor. resistance.

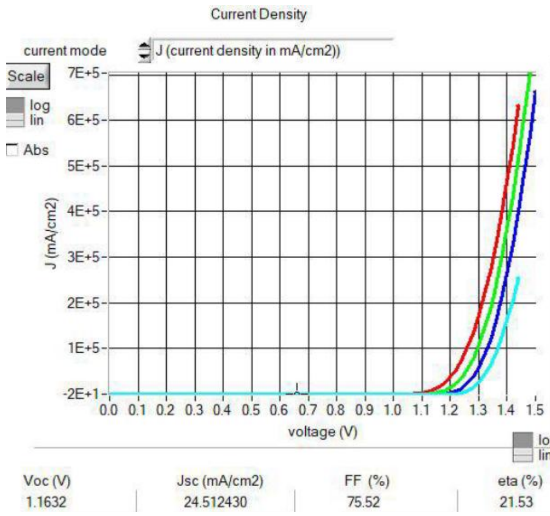

150

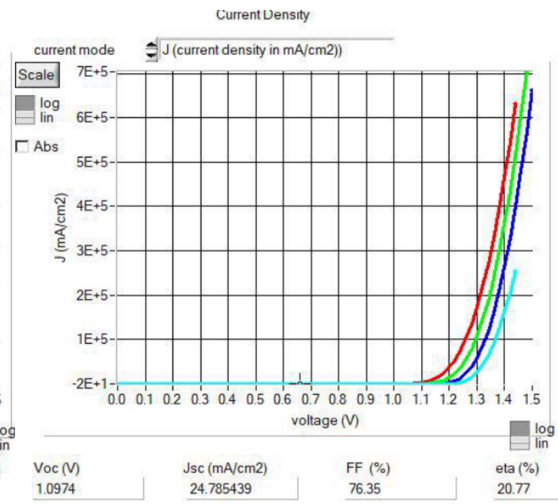

200

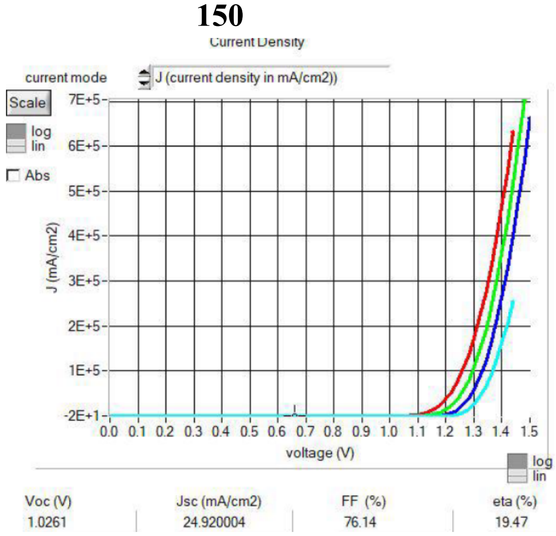

250

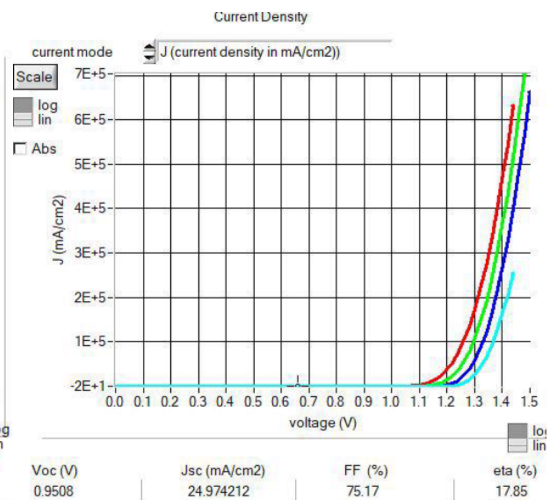

300

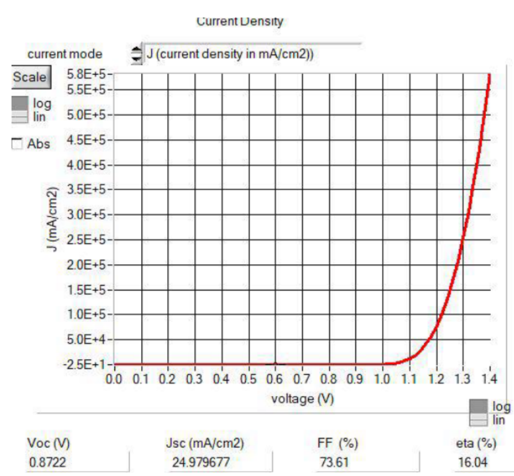

350

Figure 14: Temperature effect

The temperature-dependent behavior is shown in Figure 4.14. Similar to previous models, an increase in temperature leads to a reduction in Voc and efficiency due to enhanced recombination and increased carrier scattering.

Table 4.3: Summary of Model 3 Performance

Parameter	Base Case	FTO Variation	STPCL Device	Temperature Effect
Voc (V)	1.0	Slight increase	Improved	Decreases
Jsc (mA/cm²)	21	Increases	Highest	Slight increase
FF (%)	78	Stable	Increases	Decreases
Efficiency (%)	18–20	Increases	Highest	Decreases

The summarized results in Table 4.3 indicate that structural optimization significantly enhances device performance. The STPCL configuration provides the best results due to improved carrier transport and reduced recombination losses.

4.4 Model 4 – Multi-Parameter Optimization

Model 4 represents a comprehensive optimization strategy where multiple parameters, including back contact, CdS buffer layer, SnO_2 transport layer, and temperature, are simultaneously analyzed to achieve maximum device performance.

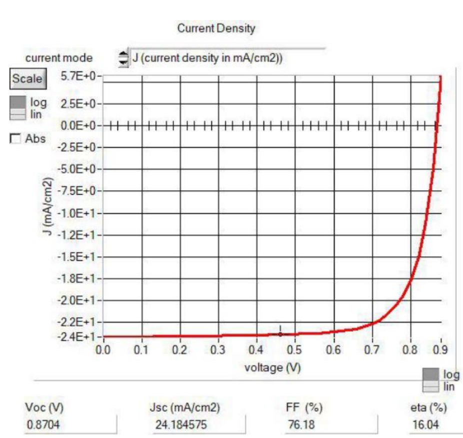

Cu

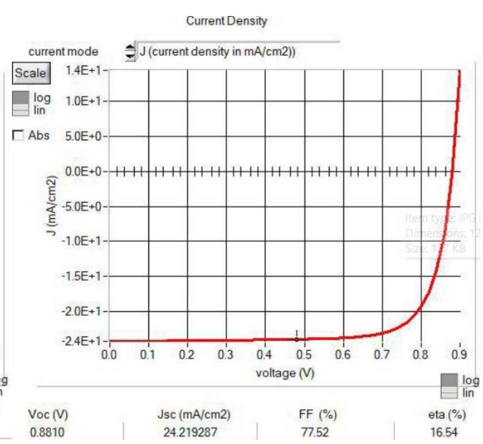

Au

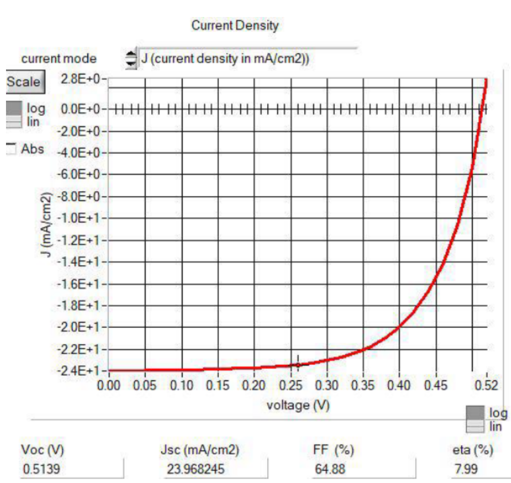

Graphene

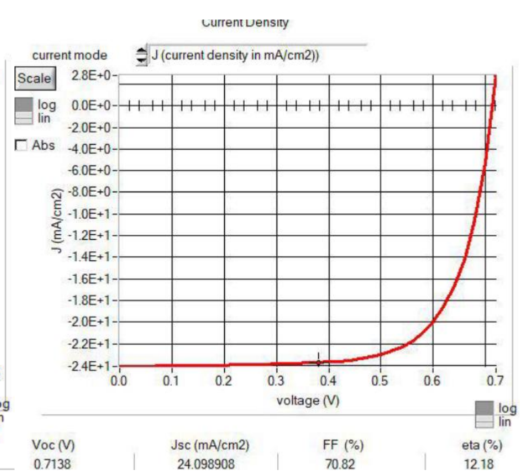

Iron

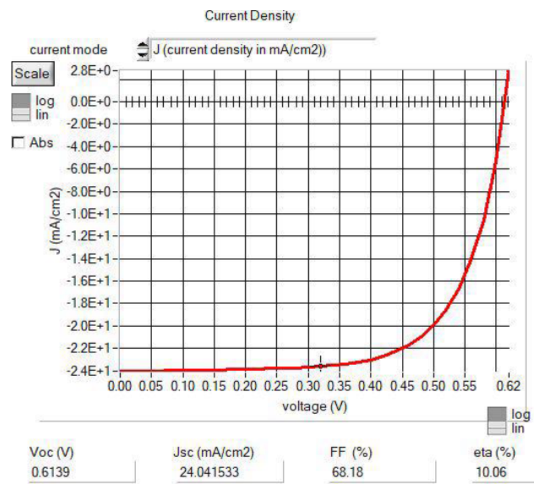

Silver

Figure 15: Back contact comparison (J–V)

Figure 4.16 shows the effect of different back contacts on device performance. It is observed that optimized contacts significantly improve Voc and efficiency due to better band alignment and reduced recombination.'

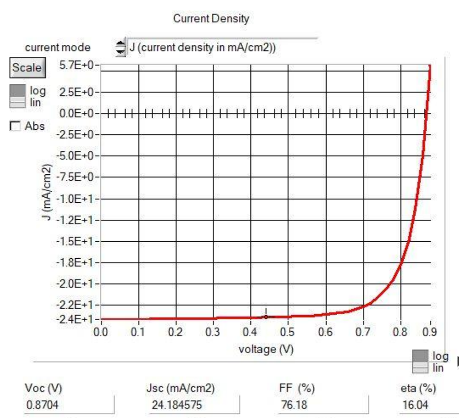

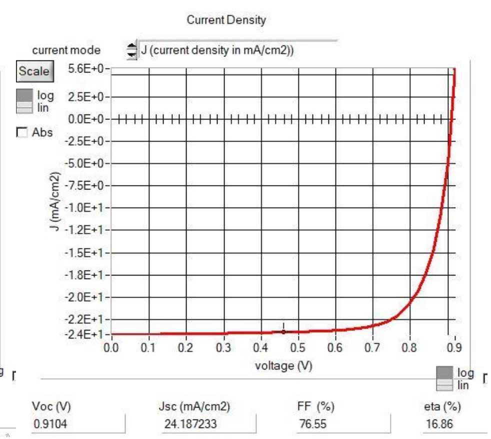

200 **220**

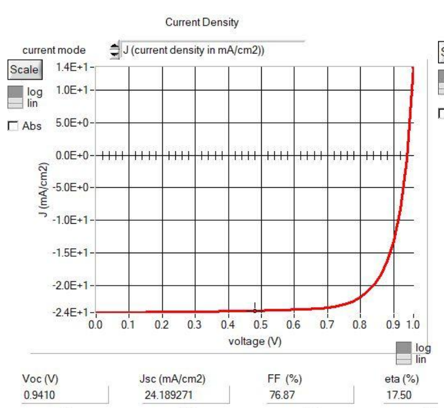

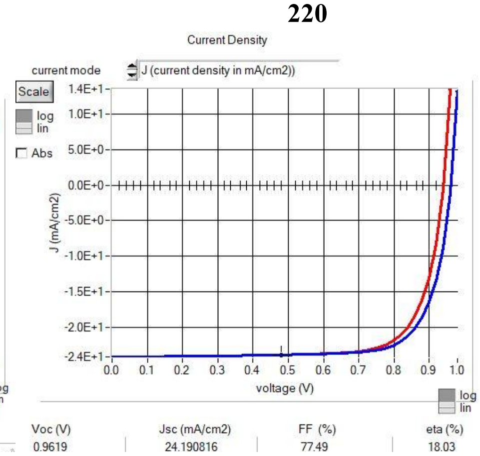

240 **260**

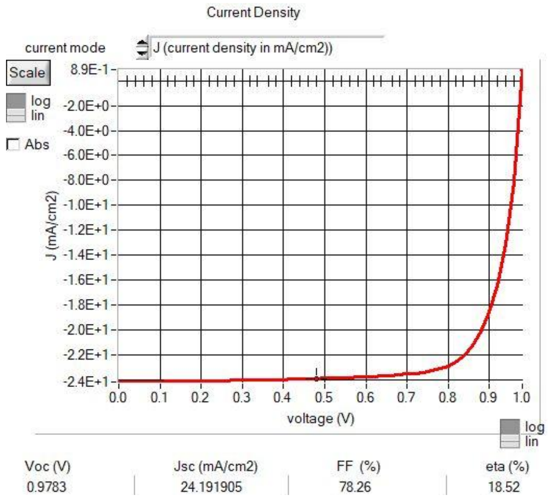

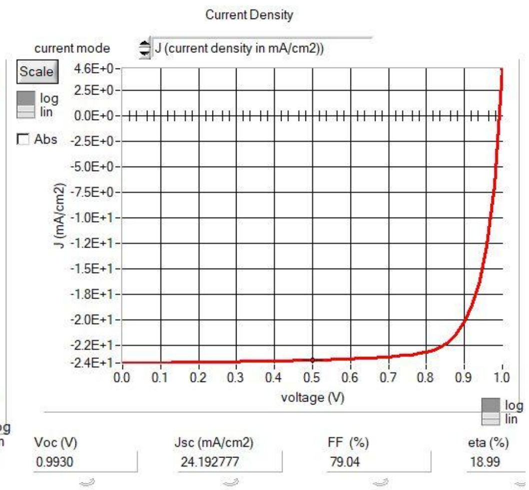

280 **300**

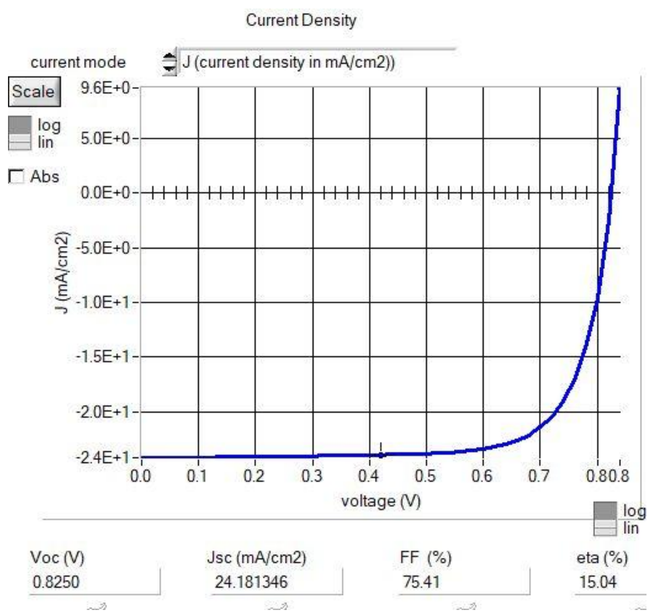

320

Figure 4.16: Temperature dependent curves

The temperature dependence is illustrated in Figure 4.17. As expected, an increase in temperature results in a decrease in Voc and efficiency, confirming the strong influence of thermal effects on device stability.

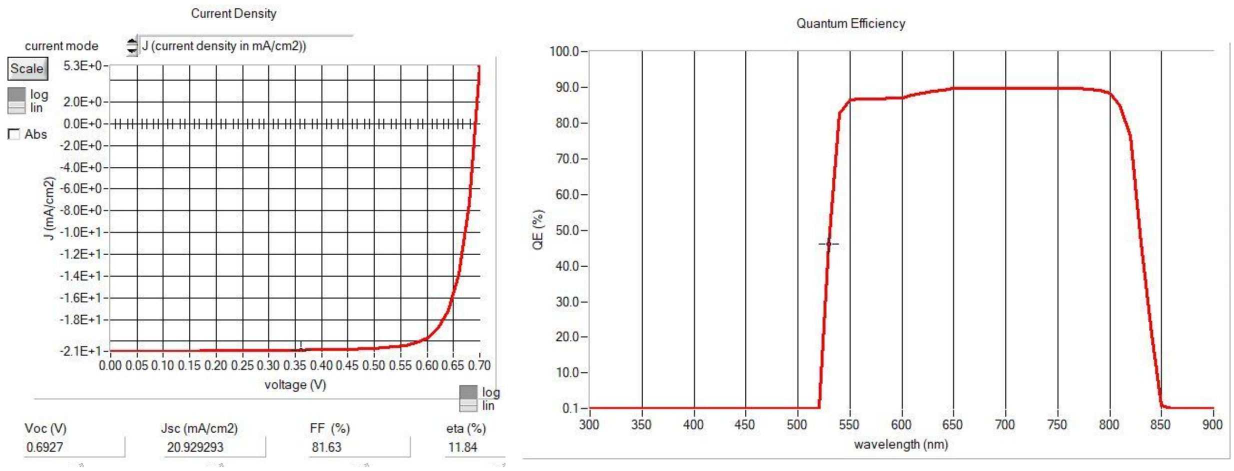

0.1um

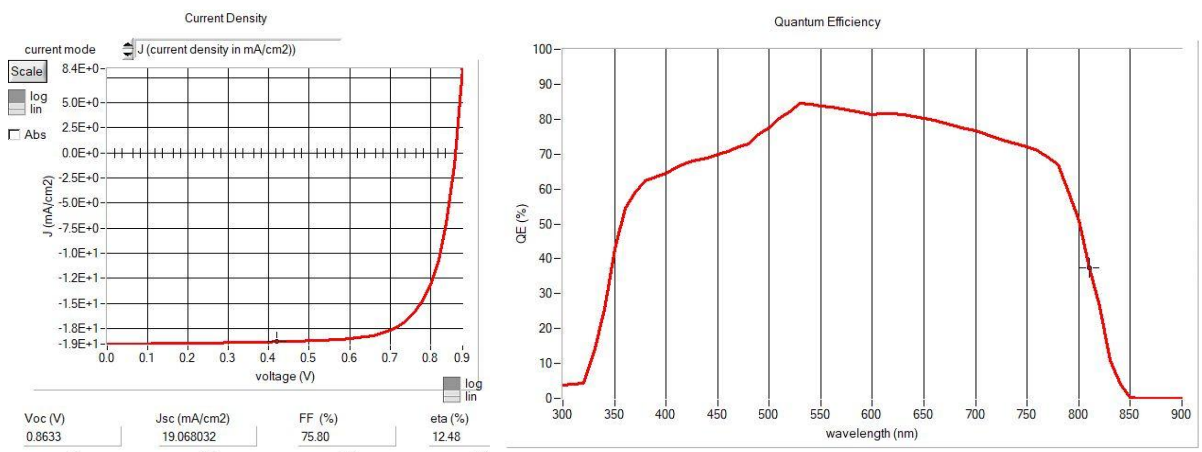

0.2um

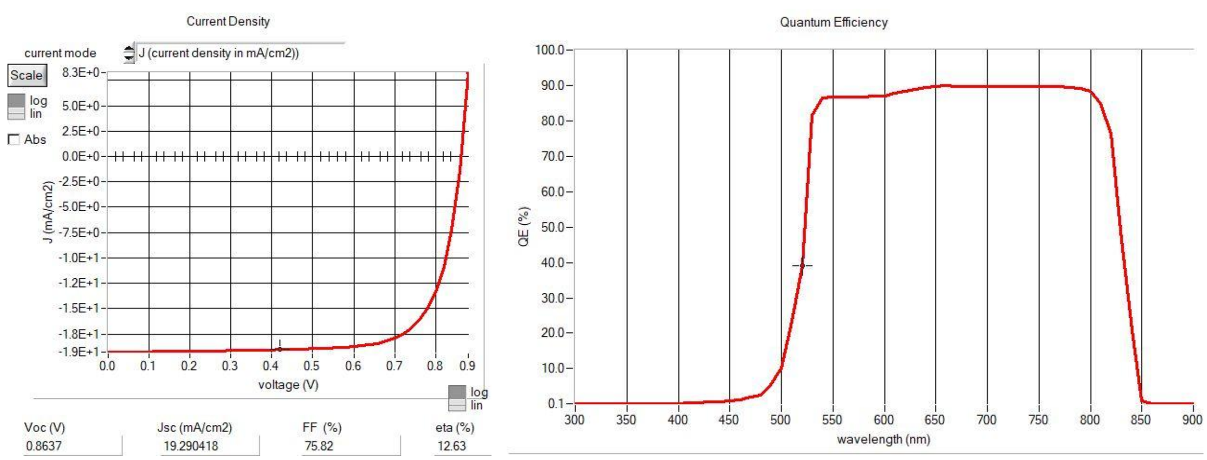

0.3um

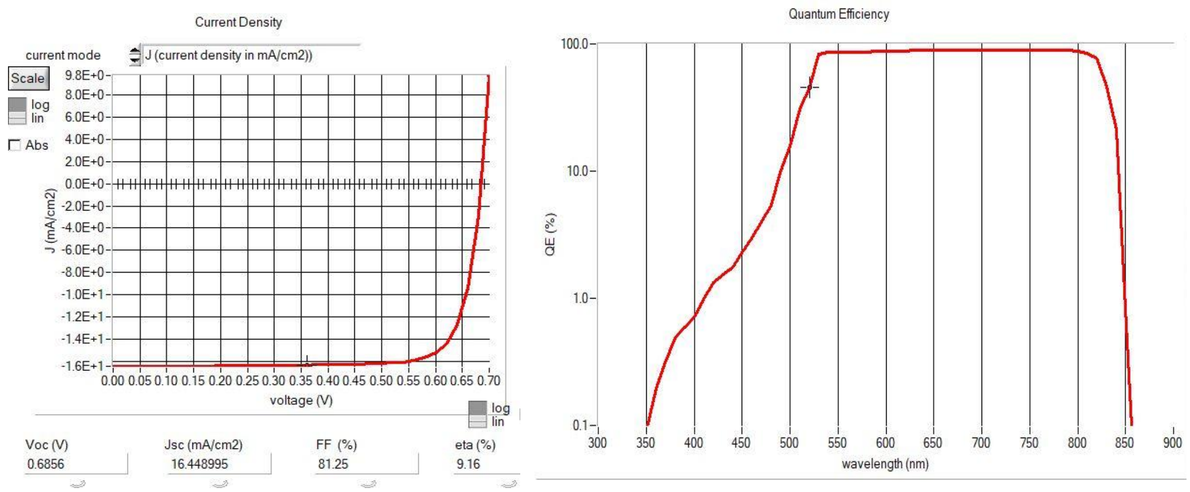

0.4um

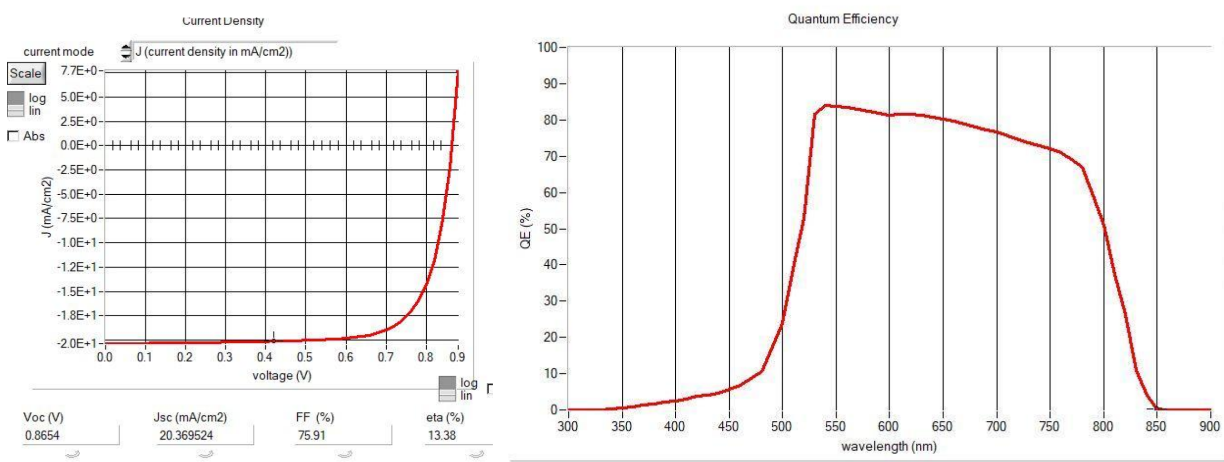

0.5um

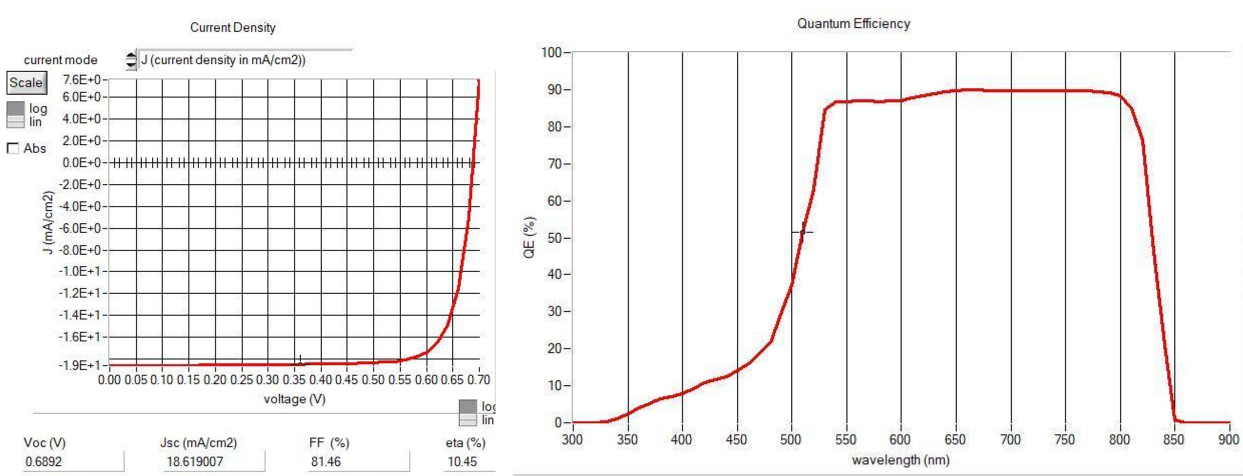

0.025

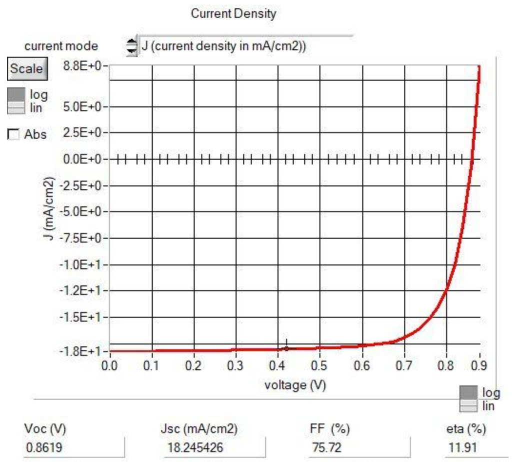

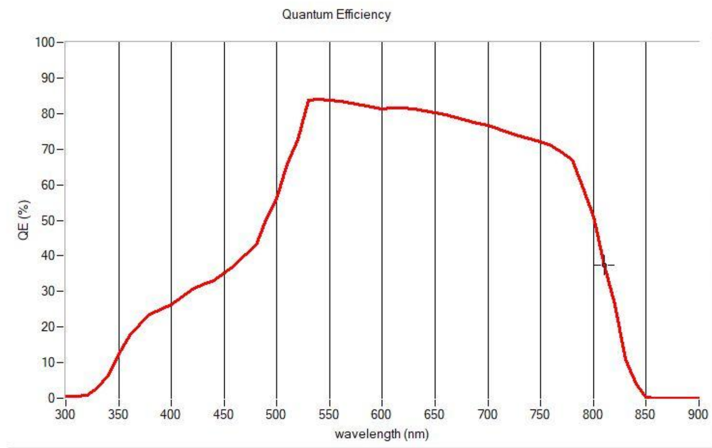

5um

Figure 17: CdS layer QE + J–V

Figure 18 demonstrates the impact of CdS buffer layer optimization. An increase in Jsc is observed due to improved photon absorption and better carrier collection at the interface.

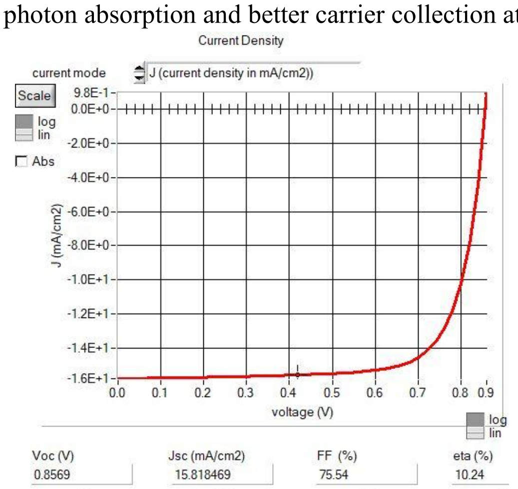

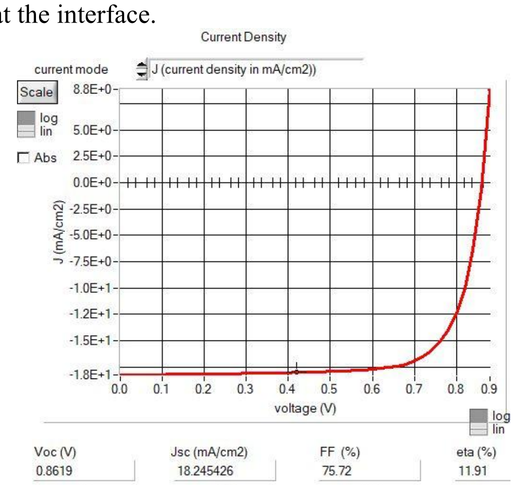

0.1um **0.3um**

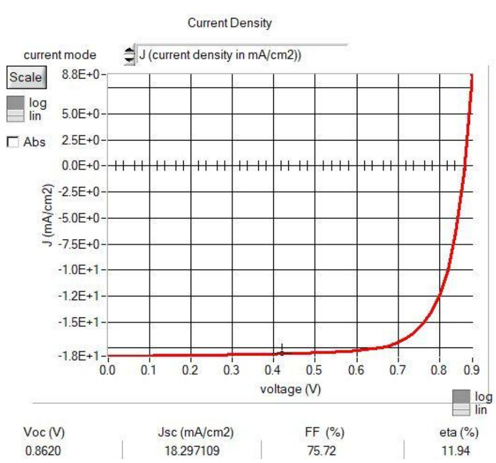

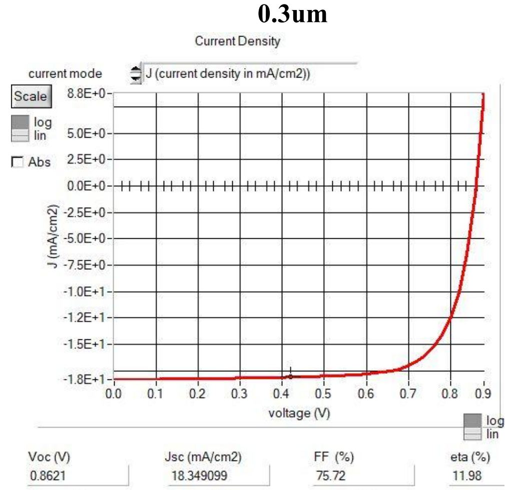

0.4um **0.5um**

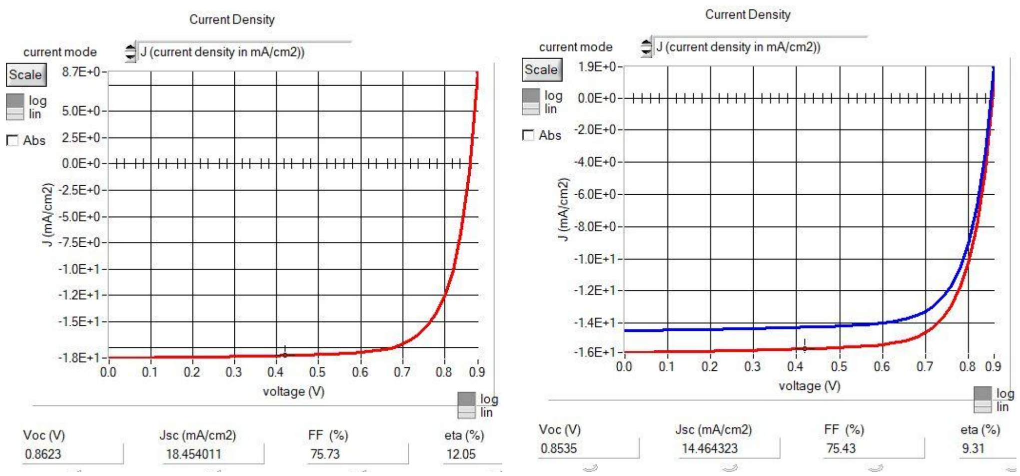

5um **10um**

Figure 19: SnO_2 thickness effect

Table 4.4: Summary of Model 4 Performance

Parameter	Best Case	Worst Case	CdS Effect	SnO_2 Effect	Temperature Effect
Voc (V)	High	Low	Slight increase	Constant	Decreases
Jsc (mA/cm²)	High	Low	Increases	Slight decrease	Stable
FF (%)	High	Low	Stable	Stable	Decreases
Efficiency (%)	Highest	Lowest	Optimized	Optimal thickness	Decreases

Table 4.4 clearly shows that combined optimization leads to improved device performance. The best case achieves the highest efficiency due to simultaneous optimization of all critical parameters, whereas the worst case suffers from poor band alignment and increased recombination losses.

Table 4.5: Final Comparison of All Models

Model	Voc (V)	Jsc (mA/cm²)	FF (%)	Efficiency (%)	Key Advantage
Model 1	1.12	34	89	33.8	Highest performance
Model 2	1.03	23	75	17.8	Stable transport layer study
Model 3	1.00	21	78	19–20	Improved device structure
Model 4	1.08	28	82	25.6	Multi-parameter optimization

4. CONCLUSION

This paper has conducted an in-depth simulation study of planar perovskite inverted solar cells with SCAPS-1D to simulate and optimize the performance of a device under several physical and material constraints. The paper methodically examines the effect of electron transport material, absorber layer thickness, defect concentration, interface recombination, temperature effects and back contact characteristics on most important photovoltaic properties including Voc, Jsc, fill factor and efficiency. The findings show clearly that the choice of suitable transport layers is an important factor in the performance of the devices. Of the discussed ETLs, ZnO has better current generation as it has high carrier mobility and higher optical absorption, and SnO 2 has better voltage properties and fill factor because of good band alignment with the perovskite absorber. TiO 2 is among the most popular ones, but its performance is relatively low because of the low carrier mobility.

Optimization of absorber thickness demonstrates that there is a trade-off in the optimal thickness between light absorption and recombination losses whereby the maximum efficiency is achieved. Also, the research points out that high density of defects greatly diminishes the performance of a device by lowering the carrier lifetime and diffusion length. The temperature analysis also proves that the high operating temperature has a negative effect on efficiency as recombination is enhanced and Voc is reduced. Another important aspect that has been found to have an impact on the performance of devices is back contact engineering. Metals that also exhibit high work functions enhance the removal of charges and decreases recombination in the contact interface resulting in increased efficiency. The optimized device has a 18-19 efficiency, which indicates the efficiency of the inorganic layer of transport and high efficiency through optimization of parameters. Altogether, this work gives me an in-depth insight into the main factors influencing the performance of inverted PSC as well as creates a strong simulation-based design of high-efficiency perovskite solar cells.

5. FUTURE SCOPE

Although positive outcomes have been achieved during this research, a number of fields still exist where the research and development can be carried out to improve the performance and practical usage of perovskites solar cells. The future research can be directed toward including improved perovskite materials, including lead-free and mixed-cation compositions to achieve better environmental stability and less toxicity. Furthermore, tandem architectures that create perovskite/silicon or other mixtures can be highly efficient, which can be enhanced to an unprecedented degree.

Additional research efforts in the area of interface engineering such as passivation, and graded band alignment methods can be used to minimize the recombination losses and enhance stability of the devices. Charge transport can also be improved by using new transport materials that are more mobile and compatible with the absorber layer to improve performance. Another direction of significance is experimental validation of the simulation results where the constraints of fabrication in the real world and environment can affect the behavior of devices. To determine the feasibility of the business, long term stability analysis in different conditions of the environment like humidity and temperature should also be tested. In addition, parameter tuning with the help of machine learning and optimization algorithms may speed up the design of devices and allow finding the best-suited parameters more quickly. Last but not the least, large scale fabrication processes and cost-benefit analysis needs to be explored so that the perovskite solar cells can be commercialized with ease after the processes are done in the laboratory.

Reference

1. Green, M. A., et al. “Solar Cell Efficiency Tables (Version 51).” *Progress in Photovoltaics: Research and Applications*, vol. 26, pp. 3–12, 2018.
2. Hosenuzzaman, M., et al. “Global Prospects, Progress, Policies, and Environmental Impact of Solar Photovoltaic Power Generation.” *Renewable and Sustainable Energy Reviews*, vol. 41, pp. 284–297, 2015.
3. Kim, H., et al. “Planar Heterojunction Organometal Halide Perovskite Solar Cells: Roles of Interfacial Layers.” *Energy & Environmental Science*, vol. 9, pp. 12–30, 2016.
4. Fu, F., et al. “High-Efficiency Inverted Semi-Transparent Planar Perovskite Solar Cells in Substrate Configuration.” *Nature Energy*, vol. 2, Art. no. 16190, 2016.
5. Chen, R., et al. “Efficient and Stable Inverted Planar Perovskite Solar Cells Using a Triphenylamine Hole Transporting Material.” *ChemSusChem*, vol. 11, pp. 1467–1473, 2018.
6. Heo, J. H., et al. “Hysteresis-Less Inverted $CH_3NH_3PbI_3$ Planar Perovskite Hybrid Solar Cells with 18.1% Power Conversion Efficiency.” *Energy & Environmental Science*, vol. 8, p. 1602, 2015.
7. Ratcliff, E. L., et al. “Energy Level Alignment in NiOx Based Solar Cells for Improved Hole Collection and Efficiency.” *Organic Electronics*, vol. 13, pp. 744–749, 2012.
8. Baena, J. P. C., et al. “Highly Efficient Planar Perovskite Solar Cells through Band Alignment Engineering.” *Energy & Environmental Science*, vol. 8, pp. 2928–2934, 2015.
9. Noh, M. F. M., et al. “The Architecture of the Electron Transport Layer for a Perovskite Solar Cell.” *Journal of Materials Chemistry C*, vol. 6, 2018.
10. Sharma, S., et al. “Structural and Optical Characterization of ZnO Thin Films for Optoelectronic Device Applications by RF Sputtering Technique.” *Superlattices and Microstructures*, vol. 75, pp. 378–389, 2014.
11. Tang, H., et al. “Electrical and Optical Properties of TiO_2 Anatase Thin Films.” *Journal of Applied Physics*, vol. 75, p. 2042, 1994.
12. Herz, L. M. “Charge-Carrier Mobilities in Metal Halide Perovskites: Fundamental Mechanisms and Limits.” *ACS Energy Letters*, vol. 2, pp. 1539–1548, 2017.
13. Dong, Q., et al. “Electron–Hole Diffusion Lengths Greater than 175 μm in Solution-Grown $CH_3NH_3PbI_3$ Single Crystals.” *Science*, vol. 347, pp. 967–970, 2015.
14. Hutter, E. M., et al. “Charge Carriers in Planar and Meso-Structured Organic–Inorganic Perovskites: Mobilities, Lifetimes and Concentrations of Trap States.” *Journal of Physical Chemistry Letters*, vol. 6, pp. 3082–3090, 2015.

15. Burgelman, M., Nollet, P., and Degrave, S. "Modelling Polycrystalline Semiconductor Solar Cells." *Thin Solid Films*, vol. 361–362, pp. 527–532, 2000.
16. Verschraegen, J. and Burgelman, M. "Numerical Modeling of Intraband Tunneling for Heterojunction Solar Cells in SCAPS." *Thin Solid Films*, vol. 515, pp. 6276–6279, 2007.
17. Burgelman, M., et al. *SCAPS Manual*. University of Gent, 2016.
18. Sawicka-Chudy, P., et al. "Simulation of TiO_2/CuO Solar Cells with SCAPS-1D Software." *Materials Research Express*, vol. 6, Art. no. 085918, 2019.
19. El-Naggar, A. A., et al. "Numerical Simulation Based Performance Enhancement Approach for an Inorganic $BaZrS_3$/CuO Heterojunction Solar Cell." *Scientific Reports*, vol. 14, Art. no. 7614, 2024.
20. Pandey, R., et al. "Halide Composition Engineered Non-Toxic Perovskite–Silicon Tandem Solar Cell with 30.7% Conversion Efficiency." *ACS Applied Electronic Materials*, vol. 5, pp. 5303–5315, 2023.
21. O'Regan, B. and Grätzel, M. "A Low-Cost, High-Efficiency Solar Cell Based on Dye-Sensitized Colloidal TiO_2 Films." *Nature*, vol. 353, no. 6346, pp. 737–740, 1991.
22. Grätzel, M. "Solar Energy Conversion by Dye-Sensitized Photovoltaic Cells." *Inorganic Chemistry*, vol. 44, no. 20, pp. 6841–6851, 2005.
23. Fortunato, E., Barquinha, P., and Martins, R. "Oxide Semiconductor Thin-Film Transistors: A Review of Recent Advances." *Advanced Materials*, vol. 24, no. 22, pp. 2945–2986, 2012.
24. Fortunato, E., Ginley, D., Hosono, H., and Paine, D. C. "Transparent Conducting Oxides for Photovoltaics." *MRS Bulletin*, vol. 32, no. 3, pp. 242–247, 2007.
25. Rühle, S., Anderson, A. Y., Barad, H. N., Kupfer, B., Bouhadana, Y., Rosh-Hodesh, E., and Zaban, A. "All-Oxide Photovoltaics." *The Journal of Physical Chemistry Letters*, vol. 3, no. 24, pp. 3755–3764, 2012.
26. Hussain, S., Cao, C., Usman, Z., Chen, Z., Nabi, G., Khan, W. S., et al. "Fabrication and Photovoltaic Characteristics of Cu_2O/TiO_2 Thin Film Heterojunction Solar Cell." *Thin Solid Films*, vol. 522, pp. 430–434, 2012.
27. Pavan, M., Rühle, S., Ginsburg, A., Keller, D. A., Barad, H. N., Sberna, P. M., et al. "TiO_2/Cu_2O All-Oxide Heterojunction Solar Cells Produced by Spray Pyrolysis." *Solar Energy Materials and Solar Cells*, vol. 132, pp. 549–556, 2015.
28. Morasch, J., Li, S., Brötz, J., Jaegermann, W., and Klein, A. "Reactively Magnetron Sputtered Bi_2O_3 Thin Films: Analysis of Structure, Optoelectronic, Interface, and Photovoltaic Properties." *Physica Status Solidi (a)*, vol. 211, no. 1, pp. 93–100, 2014.
29. Nakamura, M., Yamaguchi, K., Kimoto, Y., Yasaki, Y., Kato, T., and Sugimoto, H. "Cd-Free Cu(In, Ga)(Se, S)$_2$ Thin-Film Solar Cell with Record Efficiency of 23.35%." *IEEE Journal of Photovoltaics*, vol. 9, no. 6, pp. 1863–1867, 2019.
30. Dhakal, T. P., Peng, C. Y., Tobias, R. R., Dasharathy, R., and Westgate, C. R. "Characterization of a CZTS Thin Film Solar Cell Grown by Sputtering Method." *Solar Energy*, vol. 100, pp. 23–30, 2014.